

Chromomagnetic and chromoelectric dipole moments of quarks in the reduced 331 model

A. I. Hernández-Juárez and G. Tavares-Velasco

*Facultad de Ciencias Físico Matemáticas, Benemérita Universidad
Autónoma de Puebla, Apartado Postal 1152, Puebla, Puebla, México*

A. Moyotl

*Ingeniería en Mecatrónica, Universidad Politécnica de Puebla, Tercer Carril del Ejido Serrano s/n,
San Mateo Cuanalá, Juan C. Bonilla, Puebla, Puebla, México*

(Dated: June 3, 2022)

The one-loop contributions to the chromomagnetic dipole moment $\hat{\mu}_t(q^2)$ and electric dipole moment $\hat{d}_t(q^2)$ of the top quark are calculated within the reduced 331 model (RM331) in the general case of an off-shell gluon. It is argued that the results are gauge independent for $q^2 \neq 0$ and represent valid observable quantities. In the RM331 $\hat{\mu}_t(q^2)$ receives new contributions from two heavy gauge bosons Z' and V^+ and a new neutral scalar boson h_2 , along with a new contribution from the standard model Higgs boson via flavor changing neutral currents. The latter, which are also mediated by the Z' gauge boson and the scalar boson h_2 , can give a non-vanishing \hat{d}_t provided that there is a CP -violating phase. The analytical results are presented in terms of both Feynman parameter integrals and Passarino-Veltman scalar functions, which are useful to cross-check the numerical results. Both $\hat{\mu}_t(q^2)$ and \hat{d}_t are numerically evaluated for parameter values still allowed by the constraints from experimental data. It is found that the new one-loop contributions of the RM331 to $\hat{\mu}_t(q^2)$ are of the same order of magnitude or larger than in other standard model extensions, with the dominant contribution arising from the V^+ gauge boson for $\|q\|$ in the 30-1000 GeV interval and a mass m_V of the order of a few hundreds of GeVs. As for $\hat{d}_t(q^2)$, it receives the largest contribution from h_2 exchange and can reach values of the order of 10^{-20} , which is smaller than the contributions predicted by other standard model extensions.

PACS numbers:

I. INTRODUCTION

The anomalous magnetic dipole moment and the electric dipole moment are among those lepton properties that have stirred more interest in experimental and theoretical fields. Currently, there is a discrepancy between the theoretical standard model (SM) prediction of the muon anomalous MDM and its experimental measurement, which might be a hint of new physics [1]. On the other hand, any experimental evidence of an electric dipole moment would give a clear signal of new sources of CP violation as the SM contributions are negligibly small. With the advent of the LHC, anomalous contributions to the $\bar{t}t g$ coupling have also become the focus of interest. In analogy with the lepton electromagnetic vertex $\ell\ell\gamma$, the anomalous $\bar{q}qg$ coupling can be written as

$$\mathcal{L} = -\frac{1}{2}\bar{q}\sigma^{\mu\nu}\left(\tilde{\mu}_q + i\tilde{d}_q\gamma^5\right)T^a q G_{\mu\nu}^a, \quad (1)$$

where $\tilde{\mu}_q$ is the quark chromomagnetic dipole moment (CMDM) and \tilde{d}_q is the quark chromoelectric dipole moment (CEDM), whereas $G_a^{\mu\nu}$ is the gluon field tensor and T^a are the $SU(3)$ color generators. It is also usual to define the CMDM and CEDM in the dimensionless form [2]

$$\hat{\mu}_q \equiv \frac{m_q}{g_S}\tilde{\mu}_q, \quad (2)$$

$$\hat{d}_q \equiv \frac{m_q}{g_S}\tilde{d}_q. \quad (3)$$

On the experimental side, the search for evidences of the anomalous top quark coupling $\bar{t}t g$ is underway at the LHC [2–4]: the most recent bounds on the top quark CMDM and CEDM were obtained by the CMS collaboration [4, 5], which managed to improve the previous bounds [2] by one order of magnitude. Thus, one would expect that more tight constraints on $\hat{\mu}_t$ and \hat{d}_t could be set in the near future. As far as the theoretical predictions are concerned, in the SM the CMDM is induced at the one-loop level or higher orders via electroweak (EW) and QCD contributions, whereas the CEDM can arise up to the three-loop level [6–8]. The SM contributions to $\hat{\mu}_t$ have been already studied in [9–11], and more recently a new evaluation was presented to address some ambiguities of previous calculations

[12, 13]. Since both the top quark CMDM and CEDM could receive a considerable enhancement by new physics contributions, several calculations have been reported in the literature within the framework of extension theories such as two-Higgs doublet models (THDMs) [14], the four-generation THDM [15], models with a heavy Z' gauge boson [11], little Higgs models [16, 17], the minimal supersymmetric standard model (MSSM) [18], unparticle models [19], vector like multiplet models [20], etc. In this work we are interested in the contributions to the top quark CMDM and CEDM in the reduced 331 model [21].

The study of elementary particle models based on the $SU(3)_L \times U(1)_N$ gauge symmetry dates back to the 1970s, when it was still not clear that Weinberg's $SU(2)_L \times U(1)_Y$ model was the right theory of electroweak interactions [22]. Even after the discovery of the Z and W gauge bosons, since the electroweak gauge group is embedded into $SU(3)_L \times U(1)_N$, the so called 331 models [23, 24] became serious candidates to extend the SM and explain some issues for which it has no answer, such as the flavor problem and a possible explanation for the large splitting between the mass of the top quark and those of the remaining fermions. Several realizations of the 331 model have been proposed in the literature, which predict new fermions, gauge bosons and scalar bosons, so their phenomenologies have been considerably studied [25–30].

The minimal 331 model [23, 24] requires a very large scalar sector, which introduces three scalar triplets to give masses to the new heavy gauge bosons and one scalar sextet to endow the leptons with small masses. The complexity of this model has encouraged the appearance of alternative 331 models aimed to economize the scalar sector. In particular, the reduced 331 model (RM331) [21] only requires two scalar triplets, thereby being considerably simpler than the minimal version [31, 32]. In the RM331, the physical scalar states obtained after symmetry breaking are two neutral scalar bosons only, with the lightest one being identified with the SM Higgs boson [33], and a doubly charged one. Unlike other 331 models, no singly charged scalar arises in the RM331 [34–36]. In the gauge sector, there are one new neutral gauge boson Z' , a new pair of singly charged gauge bosons V^\pm , and a pair of doubly charged gauge bosons $U^{\pm\pm}$. Like other 331 models, the RM331 also predicts three new exotic quarks. The original RM331 is strongly disfavored by experimental data [37], though it would still be allowed as long as left-handed quarks are introduced via a particular $SU(3)_L \times U(1)_N$ representation [38, 39], which in fact would give rise to flavor changing neutral current (FCNC) effects.

The CMDM of the top quark has already been studied in the context of an early version of the 331 model [9], and more recently the contributions to the electron and muon anomalous MDM were studied in the RM331 [40] and another 331 realization [41]. In this work we present a study on the contributions of the RM331 to the top quark CMDM and CEDM. Our manuscript is organized as follows. In Section II we present a brief description of the RM331, with the Feynman rules necessary for our calculation being presented in Appendix A. The analytical calculation of the new contributions to dipole form factors of the $\bar{t}tg$ vertex are presented in Sec. III; our results in terms of Feynman parameter integrals and Passarino-Veltman scalar functions are presented in Appendix B. Section IV is devoted to a review of the current constraints on the parameter space of the model and the numerical analysis of the CMDM and CEDM of the top quark. Finally, in Sec. V the conclusions and outlook are presented.

II. BRIEF OUTLINE OF THE RM331

The number of new particles necessary to fill out the $SU(3)_L \times U(1)_N$ multiplets as well as their quantum numbers depend on the particular the model's version. We will describe briefly the main features of each sector of the RM331, focusing only on those details relevant for our calculation.

A. Scalar and gauge boson eigenstates

As far as the scalar sector is concerned, the scalar potential is given by

$$V(\chi, \rho) = \mu_1^2 \rho^\dagger \rho + \mu_2^2 \chi^\dagger \chi + \lambda_1 (\rho^\dagger \rho)^2 + \lambda_2 (\chi^\dagger \chi)^2 + \lambda_3 (\rho^\dagger \rho) (\chi^\dagger \chi) + \lambda_4 (\rho^\dagger \chi) (\chi^\dagger \rho), \quad (4)$$

where the scalar triplets transform as $\rho = (\rho^+, \rho^0, \rho^{++})^T \sim (1, 3, 1)$ and $\chi = (\chi^-, \chi^{--}, \chi^0)^T \sim (1, 3, -1)$. To induce the spontaneous symmetry breaking (SSB), the neutral scalar bosons ρ^0 and χ^0 develop non-zero vacuum expectation values (VEVs) under the shifting of the fields as

$$\rho^0, \chi^0 \rightarrow \frac{1}{\sqrt{2}} (v_{\rho, \chi} + R_{\rho, \chi} + iI_{\rho, \chi}), \quad (5)$$

which leads to the following constraints

$$\begin{aligned}\mu_1^2 + \lambda_1 v_\rho^2 + \frac{\lambda_3 v_\chi^2}{2} &= 0, \\ \mu_2^2 + \lambda_2 v_\chi^2 + \frac{\lambda_3 v_\rho^2}{2} &= 0.\end{aligned}$$

The $SU(3)_C \times SU(3)_L \times U(1)_N$ breaks down into the SM gauge group following the pattern

$$SU(3)_L \times U(1)_N \xrightarrow{\langle \chi^0 \rangle} SU(2)_L \times U(1)_Y \xrightarrow{\langle \rho^0 \rangle} U(1)_{\text{EM}}, \quad (6)$$

where v_ρ can be identified with the SM Higgs VEV v . The left over of SSB are two neutral scalar bosons and a pair of doubly charged ones $h^{\pm\pm}$ as explained below.

The mass matrix of the neutral scalar bosons in the (R_χ, R_ρ) basis is

$$\mathbf{m}_0^2 = \frac{v_\chi^2}{2} \begin{pmatrix} 2\lambda_2 & \lambda_3 t \\ \lambda_3 t & 2\lambda_1 t^2 \end{pmatrix}$$

where $t = v_\rho/v_\chi$. After diagonalization, the mass eigenstates in the limit $v_\chi \gg v_\rho$ are

$$h_1 = c_\beta R_\rho - s_\beta R_\chi, \quad h_2 = c_\beta R_\chi + s_\beta R_\rho, \quad (7)$$

with masses

$$m_{h_1}^2 = \left(\lambda_1 - \frac{\lambda_3^2}{4\lambda_2} \right) v_\rho^2, \quad (8)$$

$$m_{h_2}^2 = \lambda_2 v_\chi^2 + \frac{\lambda_3^2}{4\lambda_2} v_\rho^2, \quad (9)$$

where $\lambda_1, \lambda_2 > 0$ and $c_\beta \equiv \cos \beta \approx 1 - \lambda_3^2 v_\rho^2 / (8\lambda_2^2 v_\chi^2)$. The SM Higgs boson h can be recovered in the $s_\beta \rightarrow 0$ limit, thus h_1 must be identified with the Higgs boson discovered at the LHC. Since $m_h \simeq 125$ GeV, from Eq. (8) we obtain the relation $\lambda_1 - \lambda_3^2/(4\lambda_2) \approx 0.26$ [42]. In the case $\lambda_2, \lambda_2 < 1$, and $\lambda_3 < \lambda_2$ we obtain $m_{h_1}^2 = \lambda_1 v_\rho^2$, which recovers the SM case and thus $\lambda_1 \approx 0.26$.

In the gauge sector there are two new singly charged gauge bosons V^\pm , two doubly charged gauge bosons $U^{\pm\pm}$ and a neutral gauge bosons Z' . They acquire their masses as follows. The would-be Goldstone bosons χ^\pm are eaten by the singly charged gauge bosons, whereas a linear combination of the doubly charged would-be Goldstone bosons $\rho^{\pm\pm}$ and $\chi^{\pm\pm}$ are absorbed by the doubly charged gauge boson $U^{\pm\pm}$. Also, the orthogonal combination of $\rho^{\pm\pm}$ and $\chi^{\pm\pm}$ gives rise to a physical doubly charged scalar boson pair $h^{\pm\pm}$. Finally, the would-be Goldstone boson I_χ becomes the longitudinal components of the Z' gauge boson. Thus, the masses of the new gauge bosons at leading order at v_χ are [43]

$$m_{Z'}^2 = \frac{g^2 c_W^2}{3(1 - 4s_W^2)} v_\chi^2, \quad (10)$$

$$m_{V^\pm}^2 = \frac{g^2}{4} v_\chi^2, \quad (11)$$

$$m_{U^{\pm\pm}}^2 = \frac{g^2}{4} (v_\rho^2 + v_\chi^2). \quad (12)$$

As far as the SM gauge bosons are concerned, the would-be Goldstone bosons ρ^\pm and I_ρ endow with masses the Z and W^\pm gauge bosons, respectively.

B. Gauge and scalar boson couplings to the top quark

There are no new leptons in this model, but in the quark sector a new quark is required for each quark triplet. They transform as

$$Q_{iL} = \begin{pmatrix} d_i \\ -u_i \\ J_i \end{pmatrix}_L \sim (3, 3^*, -1/3), \quad i = 1, 2, \quad Q_{3L} = \begin{pmatrix} u_3 \\ d_3 \\ J_3 \end{pmatrix}_L \sim (3, 3, +2/3),$$

with the numbers between parentheses representing the field transformations under the $SU(3)_C \times SU(3)_L \times U(1)_N$ gauge group, whereas J_1 , J_2 and J_3 are the new exotic quarks with electric charges $Q_{J_{1,2}} = -4/3e$ and $Q_{J_3} = 5/3e$. Under this representation the theory is anomaly free [38].

1. Charged currents

In the quark sector, the charged currents relevant for our calculation are given by the following Lagrangian

$$\mathcal{L}_q^{CC} = \frac{g}{\sqrt{2}} \bar{u}_L V_{CKM}^q \gamma^\mu d_L W_\mu^+ + \frac{g}{\sqrt{2}} \bar{J}_{3L} \gamma^\mu (V_L^u)_{3a} u_{aL} V_\mu^+ + \frac{g}{\sqrt{2}} \bar{u}_{lL} (V_L^{u\dagger})_{li} \gamma^\mu J_{iL} U_\mu^{++} + \text{H.c.},$$

where the family indexes a runs over 1, 2 and 3, whereas i and l run over 1 and 2. Also $V_{CKM}^q = V_L^{u\dagger} V_L^d$ stands for the Cabibbo-Kobayashi-Maskawa matrix, with the mixing matrices V_L^u (V_L^d) transforming the left-handed up (down) quarks flavor eigenstates into their mass eigenstates. It is assumed that the new quarks are given in their diagonal basis. Note that the doubly charged gauge boson $U^{\pm\pm}$ does not couples with the top quark.

2. FCNC currents

Since the Z' gauge boson couplings to the quarks are non-universal, flavor changing neutral currents (FCNCs) are induced at the three level. The corresponding Lagrangian for the up quark sector reads

$$\mathcal{L}_{Z'}^{FCNC} = \frac{g}{2c_W \sqrt{3(1-4s_W^2)}} \left(\sum_{a=1}^3 (\bar{u}'_{aL} \gamma^\mu (1-2s_W^2) u'_{aL}) + \bar{u}'_{3L} \gamma^\mu (2s_W^2) u'_{3L} \right) Z'_\mu \quad (13)$$

where the up quarks u' are in the flavor basis. It is evident that the above Lagrangian induces FCNC at the tree level after the rotation to the mass eigenstate basis.

On the other hand, the interactions between up quarks and the neutral scalar bosons arise from

$$\mathcal{L}_S = \sum_{i,j=1}^3 \bar{u}'_{iL} \Gamma_{1ij}^u u'_{Rj} h_1 + \bar{u}'_{iL} \Gamma_{2ij}^u u'_{jR} h_2 + \text{H.c.}, \quad (14)$$

where u is an up quark triplet $u^T = (u, c, t)$ and

$$\Gamma_1^u = \frac{c_\beta}{v_\rho} \mathbf{m}^u - \frac{s_\beta}{v_\chi} \begin{pmatrix} 0 & 0 & 0 \\ 0 & 0 & 0 \\ m_{31}^u & m_{32}^u & m_{33}^u \end{pmatrix},$$

$$\Gamma_2^u = \frac{s_\beta}{v_\rho} \mathbf{m}^u + \frac{c_\beta}{v_\chi} \begin{pmatrix} 0 & 0 & 0 \\ 0 & 0 & 0 \\ m_{31}^u & m_{32}^u & m_{33}^u \end{pmatrix},$$

with \mathbf{m}^u being the quark mass matrix in the flavor basis [38]. After rotating to the mass eigenstate basis, only the terms proportional to \mathbf{m}^u are diagonalized, whereas the remaining term gives rise to FCNC couplings, which can be written as

$$\mathcal{L}_S^{FCNC} = \sum_{i,j=1}^3 (-s_\beta \bar{u}_{iL} \eta_{ij}^u u_{jR} h_1 + c_\beta \bar{u}_{iL} \eta_{ij}^u u_{jR} h_2) + \text{H.c.}, \quad (15)$$

where

$$\eta^u = \mathbf{V}_L^u \begin{pmatrix} 0 & 0 & 0 \\ 0 & 0 & 0 \\ \frac{m_{31}^u}{v_\chi} & \frac{m_{32}^u}{v_\chi} & \frac{m_{33}^u}{v_\chi} \end{pmatrix} (\mathbf{V}_R^u)^\dagger.$$

By the parametrization given in [44] for the $\mathbf{V}_{L,R}^{u,d}$ mixing matrices it is possible to obtain numerical values for the entries of the $\eta^{u,d}$ matrix. Under this framework $m_{31}^u = 0$, $m_{32}^u = 0$, and $m_{33}^u = m_t$.

III. CMDM AND CEDM OF THE TOP QUARK IN THE RM331

Apart from the pure SM contributions, at the one-loop level there are new contributions to the CMDM of the top quark arising in both the gauge and scalar sectors of the RM331. The corresponding Feynman diagrams are depicted in Fig. 1. In the gauge sector the new contributions arise from the neutral Z' gauge boson, which are induced by both diagonal and non-diagonal couplings. There are also a new contribution from the singly-charged gauge boson V^\pm , which is accompanied by the new exotic quark J_3 . As already noted, the doubly-charged gauge boson $U^{\pm\pm}$ does not couple to the top quark, but the u and c quarks only, thus there is no contribution from $U^{\pm\pm}$ to the top quark CMDM and CEDM. As for the scalar sector, the new contributions arise from the neutral scalar bosons h_1 and h_2 . The SM-like Higgs boson h_1 has its diagonal couplings modified and also gives a new contribution via its FCNC couplings, which may be induced in this model at the tree-level, whereas the new Higgs boson h_2 contributes via both diagonal and non-diagonal couplings. If complex FCNC couplings are assumed, there are also a non-vanishing CEDM at this order.

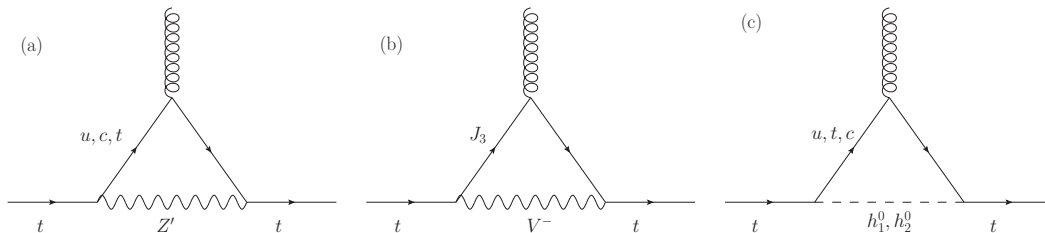


FIG. 1: New one-loop contributions of the RM331 to the CMDM and CEDM of the top quark in the unitary gauge. In the conventional linear R_ξ gauge there are additional Feynman diagrams where the gauge bosons are replaced by their associated Goldstone bosons.

We are interested in the CMDM and CEDM of a quark for an off-shell gluon. Since off-shell Green functions are not associated with an S -matrix element, they can be plagued by pathologies such as being gauge non-invariant, gauge dependent, ultraviolet divergent, etc. Along these lines, the pinch technique (PT) was meant to provide a systematic approach to construct well-behaved Green functions [45], out of which valid observable quantities can be extracted. It was later found that at the one-loop level there is an equivalence between the results found via the PT and those obtained through the background field method (BFM), as long as the Feynman gauge is used in the latter [46]. This provides a straightforward computational method to obtain gauge independent Green functions. It is thus necessary to check up on whether or not the RM331 contributions to the CMDM and CEDM of quarks are gauge independent for $q^2 \neq 0$. Nevertheless, we note that from the Feynman diagrams of Fig. 1, the gauge parameter ξ only enters into the amplitudes of the Feynman diagrams (a) and (b) via the propagators of the gauge bosons and their associated would-be Goldstone bosons. Those kind of diagrams have an amplitude that shares the same structure to those mediated by the electroweak gauge bosons Z and W in the SM, which are known to yield a gauge independent contribution to the CMDM for an off-shell gluon when the contribution of their associated would-be Goldstone bosons are added up. See for instance Ref. [12], where we performed the calculation of the electroweak contribution to the CMDM of quarks in the conventional linear R_ξ gauge and verified that the gauge parameter ξ drops out from the result. Furthermore, the dipole form factors cannot receive contributions from self-energy diagrams, which are required to cancel gauge dependent terms appearing in the monopolar terms via the PT approach. Thus both the CMDM and CEDM must be gauge independent for an off-shell gluon and thus valid observable quantities.

Below we present the analytical results of our calculation in a model-independent way, out of which the results for the RM331 and other SM extensions would follow easily. The corresponding coupling constants for the RM331 are presented in Appendix A. For the loop integration we used the Passarino-Veltman reduction method and for completeness our calculation was also performed by Feynman parametrization via the unitary gauge, which provides alternative expressions for a crosscheck of the numerical results. The Dirac algebra and the Passarino-Veltman reduction were done in Mathematica with the help of FeynCalc [47] and Package-X [48].

A. New gauge boson contributions

We first consider the generic contribution of a new gauge boson V with the following interaction to the quarks

$$\mathcal{L}^{Vqq'} = \frac{g}{c_W} \bar{q} \left(g_V^{Vqq'} - g_A^{Vqq'} \gamma^5 \right) \gamma_\mu q' V^\mu + \text{H.c.}, \quad (16)$$

where the coupling constants $g_{V,A}^{Vqq'}$ are taken in general as complex quantities. By hermicity they should obey $g_{V,A}^{Vqq'} = g_{V,A}^{Vq'q*}$.

The above interaction gives rise to a new contribution to the CMDM and CEDM via a Feynman diagram similar to that of Fig. 1(a). The corresponding contribution to the quark CMDM can be written as

$$\hat{\mu}_q^V(q^2) = \frac{G_F m_W^2}{2\sqrt{2}\pi^2 r_V^2 c_W^2} \sum_{q'} \left| g_V^{Vqq'} \right|^2 \mathcal{V}_{qq'}^V(q^2) + \left(g_V^{Vqq'} \rightarrow g_A^{Vqq'}, m'_q \rightarrow -m'_q \right), \quad (17)$$

where we introduced the auxiliary variable $r_a = m_a/m_q$ and the $\mathcal{V}_{qq'}^V(q^2)$ function is presented in Appendix B in terms of Feynman parameter integrals and Passarino-Veltman scalar functions. The notation for the second term of the right-hand side means that the first term with the indicated replacements needs to be added. As for the contribution to the quark CEDM, it can arise as long as there are flavor changing complex couplings and it is given by

$$\hat{d}_q^V(q^2) = \frac{G_F m_W^2}{\sqrt{2}\pi^2 r_V^2 c_W^2} \sum_{q'} \text{Im} \left(g_V^{Vqq'} g_A^{Vqq'*} \right) \tilde{\mathcal{D}}_{qq'}^V(q^2), \quad (18)$$

where again the $\mathcal{D}_{qq'}^V(q^2)$ function is presented in Appendix B.

From Eqs. (17) y (18) we can obtain straightforwardly the contributions to the quark CMDM and CEDM of the neutral gauge boson Z' and the singly charged gauge boson V^\pm after a proper replacement of the coupling constants and the gauge boson masses.

B. New scalar boson contributions

Following the same approach as above, we now present the generic contribution to the quark CMDM and CEDM arising from FCNC mediated by a new scalar boson S , which arise from the Feynman diagram of Fig 1(c). We consider an interaction of the form

$$\mathcal{L}^{Sqq'} = -\frac{g}{2} \bar{q} \left(G_S^{Sqq'} + G_P^{Sqq'} \gamma^5 \right) q' S + \text{H.c.} \quad (19)$$

The above scalar interaction leads to the following contribution to the quark CMDM

$$\hat{\mu}_q^S(q^2) = -\frac{G_F m_W^2}{8\sqrt{2}\pi^2} \sum_{q'} \left| G_P^{Sqq'} \right|^2 \mathcal{P}_{qq'}^S(q^2) + \left(G_P^{Sqq'} \rightarrow G_S^{Sqq'}, m'_q \rightarrow -m'_q \right), \quad (20)$$

whereas the corresponding contribution to the quark CEDM is given by

$$\hat{d}_q^S(q^2) = \frac{G_F m_W^2}{4\sqrt{2}\pi^2} \sum_{q'} \text{Im} \left(G_S^{Sqq'} G_P^{Sqq'*} \right) \tilde{\mathcal{D}}_{qq'}^S(q^2), \quad (21)$$

where the $\mathcal{P}_{qq'}^S(q^2)$ and $\tilde{\mathcal{D}}_{qq'}^S(q^2)$ functions are presented in Appendix B.

From the above expression we can obtain the contribution of the new scalar Higgs boson of the RM331 as well as the contribution of the SM Higgs boson, which in the RM331 has tree-level FCNC couplings.

IV. NUMERICAL ANALYSIS AND DISCUSSION

We now turn to the numerical analysis. The coupling constants that enter into the Feynman rules and are necessary to evaluate the CMDM and CEDM of the top quark [c.f. Eqs. (16) through (21)] are presented in Tables II and III of Appendix A. As already mentioned, the mass parameter m_{33}^u can be identified with the top quark mass [38], hence, apart from the values of the masses of the heavy gauge bosons, which depend on the VEV v_χ , we need the values of the masses of the exotic quarks, the parameters λ_2 and λ_3 , which along with v_χ define the mass of the new scalar boson m_{h_2} and the mixing angle s_β , as well as the entries of the matrices \mathbf{V}_L^u , \mathbf{K}_L and $\boldsymbol{\eta}^u$. For the latter we also require its complex phases $\phi_{\eta_{tq}^u}$ and $\phi_{\eta_{qt}^u}$. We will thus discuss the most up-to-date constraints on these parameters from current experimental data.

A. Constraints on the parameter space

The muon $g - 2$ discrepancy constrains the VEV v_χ above 2 TeV [39], which provides a bound on the values of the heavy gauge bosons masses $m_{Z'}$ and m_{V^\pm} . In our analysis we will use $v_\chi = 2$ TeV. On the other hand, for the masses of the exotic quarks, we use 1 TeV as they are expected to be of the order of the new physics scale. Following the parametrization used in [44] we can obtain the absolute values for the entries of the matrices \mathbf{V}_L^u , \mathbf{K}_L and $\boldsymbol{\eta}^u$. Finally, since the CP violation phases are expected to be very small, we assume that all the complex phases are of the order of 10^{-3} .

According to Eq. (8) the mass of the SM-like Higgs boson receives new corrections through the λ_2 and λ_3 parameters. As discussed above, the SM case is recovered when $\lambda_1 \approx 0.26$ and $\lambda_3 < \lambda_2 < 1$, thus the new corrections to m_{h_1} must lie within the experimental error of the SM Higgs boson mass $m_h = 125.10 \pm 0.14$ GeV [42]. This allows one to constrain the λ_2 and λ_3 parameters, which in turn translates into constraints on s_β and m_{h_2} once the v_χ value is fixed. We observe in Fig. 2 the allowed regions in the planes λ_2 vs λ_3 and s_β vs m_{h_2} consistent with the experimental error of the Higgs boson mass at 95% C.L. We note that for a given λ_2 , λ_3 must be about one order of magnitude below. In our calculation we use $\lambda_2 = 0.9$ and $\lambda_3 = 0.06$, though there is no great sensitivity of the top quark CMDM and CEDM to mild changes in the values of these parameters. In addition, we find that values ranging from 0.02 to 0.06 are allowed for s_β provided that $m_{h_2} \gtrsim 150$ GeV and the constraint $v_\chi \geq 2$ TeV is fulfilled.

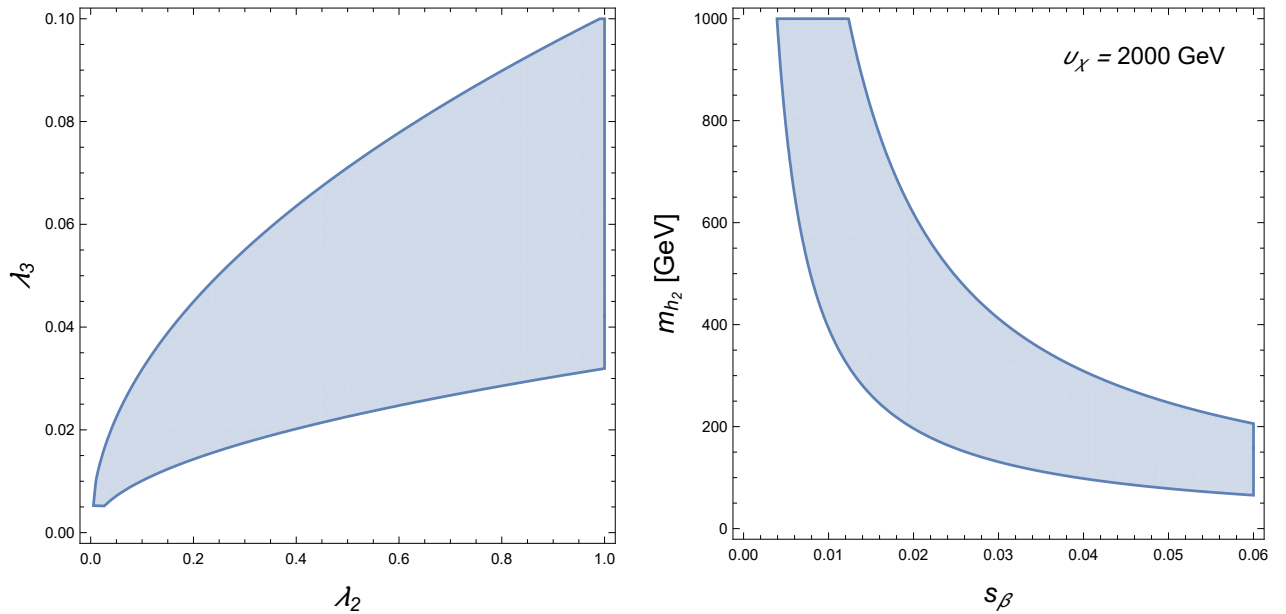


FIG. 2: Allowed areas in the planes λ_3 vs λ_2 and s_β vs m_{h_2} in agreement with the experimental error of the Higgs boson mass $m_h = 125.10 \pm 0.14$ GeV [42] at 95% C.L. We consider $\lambda_1 \approx 0.26$ and $\lambda_3 < \lambda_2 < 1$, which yield the SM limit.

We present in Table I a summary of the numerical values we will use in the numerical evaluation.

TABLE I: Numerical values of the parameters used in the evaluation of the CMDM and CEDM of the top quark in the RM331. For the entries of the matrices \mathbf{V}_L^u , \mathbf{K}_L and $\boldsymbol{\eta}^u$ we use the values obtained in [38] using the parametrization of [44], where the mass parameter m_{33} is identified with the top quark mass, and we use λ_2 and λ_3 values allowed by the experimental error in the Higgs boson mass. We also assume that the only non-negligible mixing is that arising between the third and second fermion families.

| Parameter | Value |
|--|-----------------------|
| $ (K_L)_{tc} $ | 6.4×10^{-4} |
| $ V_{33}^u $ | 1 |
| $ \eta_{tc}^u $ | 6.4×10^{-4} |
| $ \eta_{ct}^u $ | 4.62×10^{-6} |
| m_{33} | m_t |
| v_χ | 2 TeV |
| s_β | 10^{-2} |
| m_{h_2} | 150 GeV |
| $\phi_{\eta_{tc}^u}, \phi_{\eta_{ct}^u}$ | 10^{-3} |

1. Top quark CMDM

As already mentioned, in the RM331 there are new contributions to the top quark CMDM arising from the heavy gauge bosons as well as the neutral scalar bosons. The partial contributions will be referred to by the particle running into de loop of the associated Feynman diagram, with a subscript that denotes the particles to which it couples. Thus Z'_{tc} denotes the contribution of the loop with the Z' boson due to the $Z'\bar{t}c$ coupling. Since we would like to assess the size of the new physics contributions to $\hat{\mu}_t(q^2)$, we extract from our estimate the pure SM contributions, which means that for the SM Higgs boson h_1 we only include the contributions arising from the corrections to the $h_1\bar{t}t$ coupling, denoted by δh_{1tt} and from the FCNC coupling $h_1\bar{t}c$ as well.

In the left plot of Fig. 3 we show the behavior of the real parts of the partial contributions to $\hat{\mu}_t(q^2)$ as functions of $\|q\|$ for $v_\chi = 2000$ GeV, whereas the real and imaginary parts of the total contribution are shown in the right plot. We observe that there is little dependence of the real parts of the partial contributions to $\hat{\mu}_t(q^2)$ on the gluon transfer momentum, except for the δh_{1tt} contribution, which around $|q| = 600$ GeV has a flip of sign. We also note that the contribution of the V^\pm gauge boson is the largest, whereas the remaining contributions are negligible, with the h_{1tc} contribution being the smallest. Thus the total real part curve almost overlaps with that of the V^\pm contribution, with $\hat{\mu}_t(q^2)$ being of the order of $10^{-3} - 10^{-4}$. As for the imaginary parts of the partial contributions to $\hat{\mu}_t(q^2)$, they are several orders of magnitude smaller than the respective real parts, whereas the total imaginary part is negligible for $\|q\|$ below about 400 GeV and of the order of 10^{-6} for larger $\|q\|$.

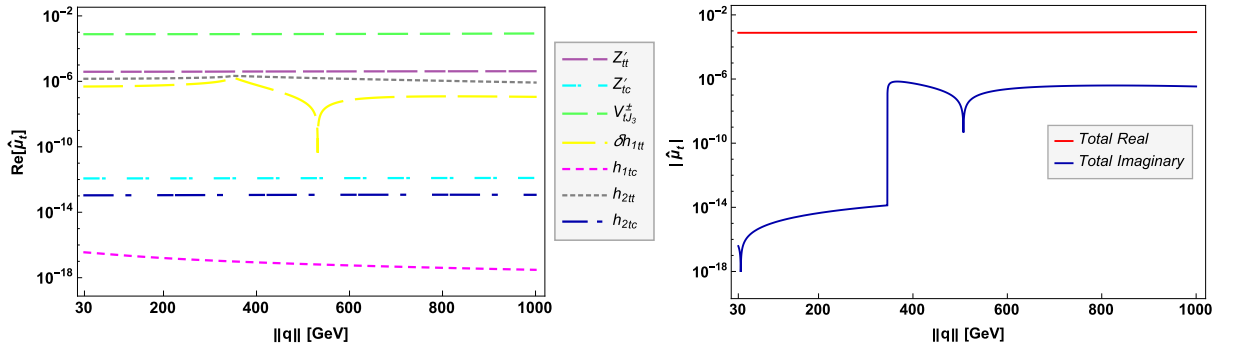


FIG. 3: Real part of the partial contributions of the RM331 to the top quark CMDM as functions of $\|q\|$ for $v_\chi=2000$ GeV (left plot). The real and imaginary parts of the total contribution are shown in the right plot. For the remaining parameters of the model we use the values of Table I.

Similar plots to those presented in Fig. 3 but now for the behavior of $\hat{\mu}_t(q^2)$ as a function of v_χ for $\|q\| = 500$ GeV are shown in Fig. 4. In this case we observe that the real parts of the partial contributions to $\hat{\mu}_t(q^2)$ show a

slight variation of about one order of magnitude when v_χ increases from 2 TeV to 10 TeV. As already noted, the V^\pm contribution yields the bulk of the total contribution to $\hat{\mu}_t$, with the real part of the latter being about three orders of magnitude larger than its imaginary part.

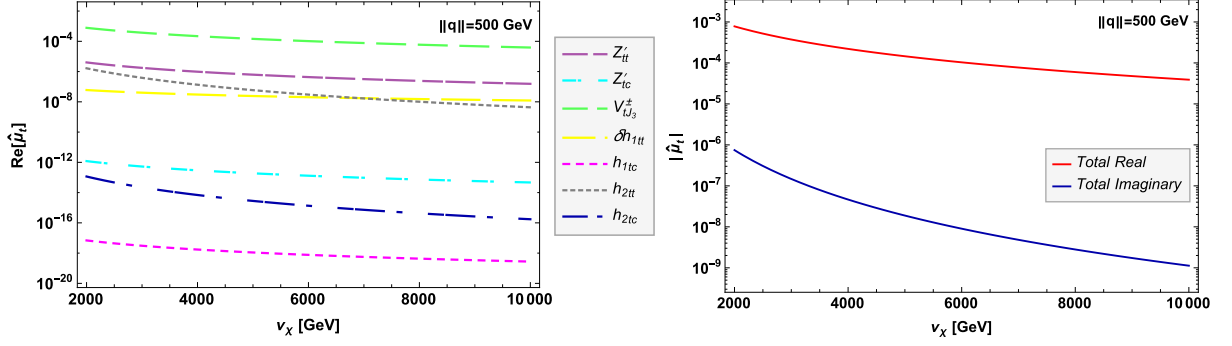


FIG. 4: The shames as in Fig. 3 but for the contributions of the RM331 to the top quark CMDM as functions of v_χ for $\|q\|=500$ GeV.

In summary, the real part of the new contribution of the RM331 can be of the same order of magnitude than the real part of the pure electroweak contribution of the SM [12]. Therefore the RM331 could give a contribution larger than the ones arising in other extension models (see for instance Ref. [15] for a compilation of predictions of the top quark CMDM in several extension models). However, the imaginary part of the RM331 contribution is smaller than its real part, being three or more orders of magnitude smaller. We would like to point out that there is no appreciable variation in the magnitude of $\hat{\mu}_t$ for mild changes in the parameters of the model.

2. Top quark CEDM

A potential new source of CP violation can arise in the RM331 through the FCNC couplings mediated by the neutral scalar bosons, which are proportional to the entries of the non-symmetric complex mixing matrix η^u [38], thereby allowing the presence of a non-zero CEDM. We show in Fig. 5 the contour lines of the real part (left plot) and the imaginary part (right plot) of the total contribution of the RM331 to the CEDM of the top quark in the v_χ vs $\|q\|$ plane for the parameter values of Table I. The dominant and essentially total contribution to \hat{d}_t arises from the loop with the new scalar boson h_2 , which can be as large as 10^{-19} , whereas the contribution from the h_1 scalar boson is three or more orders of magnitude smaller. We also observe that the imaginary part of d_t decreases as v_χ and $\|q\|$ increase, while the real part remains almost constant when $\|q\|$ increases. For $v_\chi \gg 4000$ GeV, the RM331 contribution to the CEDM of the top quark is expected to be below the 10^{-20} level, which seems to be much smaller than the values predicted in other extension models. Again, for a compilation of estimates of the top quark CEDM in several extension models we refer the reader to Ref. [15]. To our knowledge there is no previous estimate of the top quark CEDM in 331 models.

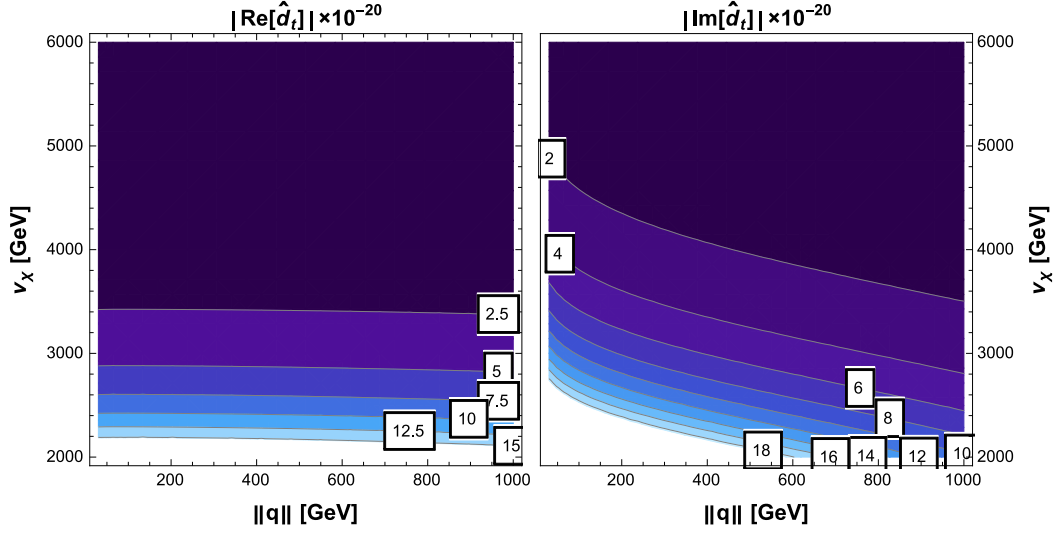


FIG. 5: Real part (left plot) and imaginary part (right plot) of the total contribution to the CEDM of the top quark in the RM331 in the plane v_χ vs $\|q\|$. We use the parameter values of Table I.

V. CONCLUSIONS

We present a calculation of the one-loop contributions to the CMDM and CEDM, $\hat{\mu}_t(q^2)$ and $\hat{d}_t(q^2)$, of the top quark in the framework of the RM331, which is an economic version of the so-called 331 models with a scalar sector comprised by two scalar triplets only. We have considered the general case of an off-shell gluon as it has been pointed out before that the QCD contribution to $\hat{\mu}_t(q^2)$ is infrared divergent and the CMDM has no physical meaning for $q^2 = 0$. We argue that the results are gauge independent for $q^2 \neq 0$ and represent valid observable quantities since the structure of the gauge boson contributions are analogue to those arising in the SM. Apart from the usual SM contributions, the CMDM of the top quark receives new contributions from two new heavy gauge bosons Z' and V^+ as well as one new neutral scalar boson h_2 , along with a new contribution from the neutral scalar boson h_1 , which must be identified with the 125 GeV scalar boson detected at the LHC. This model also predicts tree-level FCNCs mediated by the Z' gauge boson and the two neutral scalar bosons h_1 and h_2 , which at the one-loop level can also give rise to a non-vanishing CEDM provided that there is a CP -violating phase. The analytical results are presented in terms of both Feynman parameter integrals and Passarino-Veltman scalar functions, which are useful to cross-check the numerical results. We present an analysis of the region of the parameter space of the model consistent with experimental data and evaluate the CMDM and CEDM of the top quark for parameter values still allowed. It is found that the new one-loop contributions of the RM331 to $\hat{\mu}_t(q^2)$ are of the same order of magnitude or larger than in other SM extensions, with the dominant contribution arising from the V^+ gauge boson and all the remaining contributions being considerably smaller. It is also found that there is little dependence of $\mu_t(q^2)$ on $\|q\|$ in the 30-1000 GeV interval for a mass m_V of the order of a few hundreds of GeV. As far as the CEDM of the top quark is concerned, it is mainly induced by the loop with h_2 exchange and can reach values of the order of 10^{-20} for realistic values of the CP -violating phases. Such a contribution is smaller than the ones predicted by other SM extensions.

Acknowledgments

We acknowledge support from Consejo Nacional de Ciencia y Tecnología and Sistema Nacional de Investigadores. Partial support from Vicerrectoría de Investigación y Estudios de Posgrado de la Benémerita Universidad Autónoma de Puebla is also acknowledged.

Appendix A: Feynman rules

We now present in Tables II and III the coupling constants that enter into the Feynman rules [38, 40, 43] that follow from Eqs. (16) and (19) and are necessary for the evaluation of the CMDM and CEDM of the top quark in the RM331.

TABLE II: Coupling constants for the interactions between gauge bosons and quarks in the RM331. We follow the notation of Lagrangian (16). Here $(K_L)_{tq}$ are entries of the complex mixing matrix \mathbf{K}_L , where the subscript q runs over u and c . This matrix is in terms of the unitary complex matrix \mathbf{V}_L^u that diagonalizes the mass matrix of up quarks, and can be written as $(K_L)_{tq} = (V_L^u)^*_{tq}(V_L^u)_{qt}$. Here $h_W = 1 - 4s_W^2$.

| Coupling | $g_V^{Vqq'}$ | $g_A^{Vqq'}$ |
|-----------------|--|--|
| $Z'\bar{t}t$ | $\frac{1-2s_W^2}{2\sqrt{12}h_W}$ | $\frac{1-2s_W^2}{2\sqrt{12}h_W}$ |
| $Z\bar{t}q$ | $\frac{s_W^2}{\sqrt{12}h_W}(K_L)_{tq}$ | $\frac{s_W^2}{\sqrt{12}h_W}(K_L)_{tq}$ |
| $V^-\bar{t}J_3$ | $\sqrt{2}c_W(V_L^u)_{33}$ | $\sqrt{2}c_W(V_L^u)_{33}$ |

TABLE III: Coupling constants for the interactions between scalar bosons and quarks necessary for the evaluation of the one-loop contributions to the CMDM and CEDM in the RM331. We follow the notation of Lagrangian (19). Here $(\eta^u)_{tq}$ are entries of the complex mixing matrix $\boldsymbol{\eta}^u$, where the subscript q runs over u and c . This matrix is given in terms of the unitary complex matrices \mathbf{V}_L^u and \mathbf{V}_L^d that diagonalize the mass matrix of up quarks, and can be written as $(\eta^u)_{tq} = (V_L^u)_{tq}(V_R^u)^*_{tq}$ and $(\eta^u)^*_{qt} = (V_L^u)^*_{tq}(V_R^u)_{qq}$ since the matrix S_U is not symmetric.

| | $G_S^{Sqq'}$ | $G_P^{Sqq'}$ |
|---------------|--|--|
| $H_1\bar{t}t$ | $\frac{m_t}{m_W}\left(c_\beta - \frac{v_\rho}{v_\chi}s_\beta\right)$ | - |
| $H_1\bar{t}q$ | $-\frac{s_\beta v_\rho m_{33}}{v_\chi m_W}((\eta^u)_{tq} + (\eta^u)^*_{qt})$ | $-\frac{s_\beta v_\rho m_{33}}{v_\chi m_W}((\eta^u)_{tq} - (\eta^u)^*_{qt})$ |
| $H_2\bar{t}t$ | $\frac{m_t}{m_W}\left(s_\beta - \frac{v_\rho}{v_\chi}c_\beta\right)$ | - |
| $H_2\bar{t}q$ | $\frac{c_\beta v_\rho m_{33}}{v_\chi m_W}((\eta^u)_{tq} + (\eta^u)^*_{qt})$ | $\frac{c_\beta v_\rho m_{33}}{v_\chi m_W}((\eta^u)_{tq} - (\eta^u)^*_{qt})$ |

Appendix B: Analytical results for the loop integrals

In this appendix we present the loop integrals appearing in Eqs. (17), (18), (20), and (21) in terms of Feynman parameter integrals and Passarino-Veltman scalar functions both for non-zero and zero q^2 . We have verified that all the ultraviolet divergences cancel out. Furthermore, all the results are finite for $q^2 = 0$ contrary to the QCD contribution.

1. Feynman parameter integrals

The $\mathcal{V}_{qq'}^V(q^2)$ function of Eq. (17) can be written as

$$\mathcal{V}_{qq'}^V(q^2) = \int_0^1 \int_0^{1-u} \frac{dudv}{\Delta_V} \left[2(u-1)^2u + (1-r_{q'}) (2\hat{q}^2 uv(u+v-1) + (3u-1)\Delta_V \log(\Delta_V)) \right. \\ \left. - r_{q'}(u-1)^2(2u-1) - (2r_{q'}^2(u-1)^2 + r_V^2 u(u+3)) + r_{q'}(r_{q'}^2(u-1)^2 - r_V^2(u-5)u) \right], \quad (\text{B1})$$

where $\Delta_V = u((u-1) + r_V^2) - r_{q'}^2(u-1) + \hat{q}^2 v(u+v-1)$, with $\hat{q}^2 = q^2/m_q^2$ and $r_a = m_a/m_q$.

For $q^2 = 0$ we obtain

$$\mathcal{V}_{qq'}^V(0) = \int_0^1 \frac{udu}{r_V^2(u-1) - u((u-1) + r_{q'}^2)} \left[u^2((1-r_{q'})^2 + 2r_V^2) - u(2r_V^2(3-2r_{q'}) + (1+r_{q'})(1-r_{q'})^2) + 4r_V^2(1-r_{q'}) \right]. \quad (\text{B2})$$

As far as the $\tilde{\mathcal{D}}_{qq'}^V(q^2)$ function of Eq. (18), it is given by

$$\tilde{\mathcal{D}}_{qq'}^V(q^2) = r_{q'} \int_0^1 \int_0^{1-u} \frac{dudv}{\Delta_V} \left[(3u-1)\Delta_V \log(\Delta_V) + (2u+1)(u-1)^2 - r_{q'}^2(u-1)^2 + u(r_V^2(u-5) + 2\hat{q}^2 v(u+v-1)) \right], \quad (\text{B3})$$

which leads to

$$\tilde{\mathcal{D}}_{qq'}^V(0) = r_{q'} \int_0^1 \frac{u(u(1-r_{q'}^2) + 4r_V^2(u-1))}{u((u-1) + r_{q'}^2) - r_V^2(u-1)} du. \quad (\text{B4})$$

The $\mathcal{P}_{qq'}^S(q^2)$ function of Eq. (20) is

$$\mathcal{P}_{qq'}^S(q^2) = \int_0^1 \int_0^{1-u} \frac{(u-1)(u-r_{q'})}{u((u-1) + r_S^2) - r_{q'}^2(u-1) + \hat{q}^2 v(u+v-1)} dudv, \quad (\text{B5})$$

which for $q^2 = 0$ simplifies to

$$\mathcal{P}_{qq'}^S(0) = \int_0^1 \frac{u^2((1-u) - r_{q'})}{u((u-1) + r_S^2) - r_S^2(u-1)} du. \quad (\text{B6})$$

Finally, the loop function of Eq. (21) reads

$$\tilde{\mathcal{D}}_{qq'}^S(q^2) = \int_0^1 \int_0^{1-u} \frac{r_{q'}(u-1)}{u((u-1) + r_S^2) - r_{q'}^2(u-1) + \hat{q}^2 v(u+v-1)} dudv, \quad (\text{B7})$$

which yields

$$\tilde{\mathcal{D}}_{qq'}^S(0) = \int_0^1 \frac{r_{q'}(1-u)^2}{(1-u)(r_{q'}^2 - u) + r_S^2 u} du. \quad (\text{B8})$$

2. Passarino-Veltman results

We now present the results for the loop functions in terms of Passarino-Veltman scalar functions, which can be numerically evaluated readily with the help of the LoopTools [49] and Collier packages [50]. We introduce the following notation for the two- and three-point scalar functions in the usual notation:

$$B_a = B_0(0, m_a^2, m_a^2), \quad (\text{B9})$$

$$B_{q'b} = B_0(m_q^2, m_{q'}^2, m_b^2), \quad (\text{B10})$$

$$B_{\hat{q}q'} = B_0(\hat{q}^2, m_{q'}^2, m_{q'}^2), \quad (\text{B11})$$

$$C_a = m_q^2 C_0(m_q^2, m_q^2, q^2, m_{q'}^2, m_a^2, m_{q'}^2). \quad (\text{B12})$$

for $a = V, S, q'$ and $b = V, S$. We also define $\delta_b = 1 - r_b$ and $\chi_b = 1 + r_b$.

For non-zero q^2 , the loop functions of Eqs. (17) and (18) are given by

$$\begin{aligned} \mathcal{V}_{qq'}^V(q^2) = & \frac{1}{(\hat{q}^2 - 4)^2} \left[(\hat{q}^2 - 4) (r_{q'}^2 - r_V^2 + 1) (\delta_{q'}^2 + 2r_V^2) + (\hat{q}^2 - 4) (\delta_{q'}^2 + 2r_V^2) (r_{q'}^2 B_{q'} - r_V^2 B_V) \right. \\ & - \left(\delta_{q'}^2 \chi_{q'} ((\hat{q}^2 - 10) r_{q'} + \hat{q}^2 + 2) + r_V^2 (\hat{q}^2 (r_{q'} - 3)^2 - 2r_{q'} (5r_{q'} - 6) - 18) - 2 (\hat{q}^2 - 10) r_V^4 \right) B_{q'V} \\ & + \left(\delta_{q'}^2 (2\hat{q}^2 r_{q'} - 2r_{q'} (3r_{q'} + 4) + \hat{q}^2 + 2) - 2r_V^2 (\hat{q}^2 (4r_{q'} - 5) + r_{q'} (3r_{q'} - 10) + 11) + 12r_V^4 \right) B_{\hat{q}q'} \\ & + 2 \left(\delta_{q'}^3 \chi_{q'}^2 (3r_{q'} - \hat{q}^2 + 1) + \delta_{q'} r_V^2 ((5\hat{q}^2 - 8) r_{q'}^2 - (\hat{q}^2 - 4) r_{q'} - 2 ((\hat{q}^2 - 4) \hat{q}^2 + 6)) \right. \\ & \left. \left. - r_V^4 (4\hat{q}^2 (r_{q'} - 2) - (10 - 9r_{q'}) r_{q'} - 17) + 6r_V^6 \right) C_{q'V} \right], \end{aligned} \quad (\text{B13})$$

and

$$\tilde{\mathcal{D}}_{qq'}^V(q^2) = \frac{r_{q'}}{\hat{q}^2 - 4} \left[(r_{q'}^2 - 4r_V^2 - 1) (B_{q'V} - B_{\hat{q}q'}) + (r_V^2 (2\hat{q}^2 - 5r_{q'}^2 - 3) + (r_{q'}^2 - 1)^2 + 4r_V^4) C_{q'V} \right]. \quad (\text{B14})$$

As far as the results for $q^2 = 0$ are concerned, they read

$$\begin{aligned} \mathcal{V}_{qq'}^V(0) = & \frac{1}{r_V^2 - \chi_{q'}^2} \left[8r_V^6 - 4(r_{q'} (3r_{q'} + 2) + 2) r_V^4 + 2(r_{q'} (r_{q'} (2r_{q'} + 7) + 4) - 5) r_V^2 \right. \\ & + 2(r_{q'}^2 - 1)^2 (2r_{q'} \chi_{q'} + 1) - \left(4\delta_{q'}^2 r_{q'} \chi_{q'}^3 + 4r_{q'} \chi_{q'}^2 r_V^2 - 4(r_{q'} (3r_{q'} + 2) + 3) r_V^4 + 8r_V^6 \right) B_{q'V} \\ & \left. - \left(4\delta_{q'} r_{q'} \chi_{q'}^2 r_V^2 + 4(r_{q'} (r_{q'} + 2) + 3) r_V^4 - 8r_V^6 \right) B_V + 4r_{q'} (\delta_{q'}^2 \chi_{q'}^3 + r_{q'} \chi_{q'}^2 r_V^2 - 2r_{q'} r_V^4) B_{q'} \right], \end{aligned} \quad (\text{B15})$$

and

$$\begin{aligned} \tilde{\mathcal{D}}_{qq'}^V(0) = & \frac{r_{q'}}{(1 - (r_{q'} - r_V)^2)(1 - (r_{q'} + r_V)^2)} \left[(r_{q'}^2 - r_V^2 - 1) (4r_V^4 - (5r_{q'}^2 + 3) r_V^2 + (r_{q'}^2 - 1)^2) \right. \\ & + \left(4r_{q'}^2 r_V^4 + (-5r_{q'}^4 + 4r_{q'}^2 + 1) r_V^2 + (r_{q'}^2 - 1)^3 \right) B_{q'} + \left((5r_{q'}^2 + 3) r_V^4 - (r_{q'}^2 - 1)^2 r_V^2 - 4r_V^6 \right) B_V \\ & \left. - \left(3(3r_{q'}^2 + 1) r_V^4 - 6r_{q'}^2 (r_{q'}^2 - 1) r_V^2 + (r_{q'}^2 - 1)^3 - 4r_V^6 \right) B_{q'V} \right]. \end{aligned} \quad (\text{B16})$$

The loop functions of Eqs. (20) and (21) are given by

$$\begin{aligned} \mathcal{P}_{qq'}^S(q^2) = & \frac{1}{(\hat{q}^2 - 4)^2} \left[(4 - \hat{q}^2) (r_{q'}^2 - r_S^2 + 1) + (\hat{q}^2 (2r_{q'} - 1) + 6r_{q'}^2 - 8r_{q'} - 6r_S^2 - 2) B_{\hat{q}q'} \right. \\ & + \left(2\delta_{q'}^2 \chi_{q'} (1 - 3r_{q'} - \hat{q}^2) + 2r_S^2 (\hat{q}^2 (r_{q'} - 2) + 6r_{q'}^2 - 4r_{q'} + 2) - 6r_S^4 \right) C_{q'S} \\ & \left. + \left(\delta_{q'} ((\hat{q}^2 - 10) r_{q'} - \hat{q}^2 - 2) - (\hat{q}^2 - 10) r_S^2 \right) B_{q'S} + (\hat{q}^2 - 4) (r_S^2 B_S - r_{q'}^2 B_{q'}) \right], \end{aligned} \quad (\text{B17})$$

and

$$\mathcal{D}_{qq'}^S(q^2) = \frac{r_{q'}}{\hat{q}^2 - 4} \left[B_{q'S} - B_{\hat{q}q'} + (r_{q'}^2 - r_S^2 - 1) C_{q'S} \right]. \quad (\text{B18})$$

For $q^2 = 0$ we obtain

$$\begin{aligned} \mathcal{P}_{qq'}^S(0) = & \frac{1}{2(\chi_{q'} - r_S)(r_{q'} + \chi_S)} \left[(4r_{q'}^2 + 2r_{q'} - 1) r_S^2 - 2r_{q'}^4 - 2r_{q'}^3 + r_{q'}^2 - 2r_S^4 - 1 \right. \\ & \left. + 2(\delta_{q'} r_{q'} \chi_{q'}^2 - r_{q'} (2r_{q'} + 1) r_S^2 + r_S^4) B_{q'S} + 2r_{q'} (r_{q'} r_S^2 - \delta_{q'} \chi_{q'}^2) B_{q'} + 2r_S^2 (r_{q'}^2 + r_{q'} - r_S^2) B_S \right], \end{aligned} \quad (\text{B19})$$

and

$$\begin{aligned} \mathcal{D}_{qq'}^S(0) = & \frac{1}{(1 - (r_{q'} - r_S)^2)(1 - (r_{q'} + r_S)^2)} \left[(1 - r_{q'}^2 + r_S^2)^2 + (r_S^2 (1 - r_{q'}^2 + r_S^2)) (B_S - B_{q'S}) \right. \\ & \left. + (2r_S^2 - (1 - r_{q'}^2 + r_S^2) (1 - r_{q'}^2)) (B_{q'S} - B_{q'}) \right]. \end{aligned} \quad (\text{B20})$$

3. Two-point scalar functions

In closing we present the closed form solutions for the two-point Passarino-Veltman scalar functions appearing in the calculation. The three-point scalar functions are too lengthy to be shown here.

$$B_0(0, m_a^2, m_a^2) = -\log\left(\frac{m_a^2}{\mu^2}\right) + \frac{1}{\epsilon} + \log(4\pi) - \gamma_E, \quad (\text{B21})$$

$$B_0(\hat{q}^2, m_{q'}^2, m_{q'}^2) = \frac{\sqrt{\hat{q}^2 - 4r_{q'}^2}}{|\hat{q}|} \log\left(\frac{|\hat{q}| \sqrt{\hat{q}^2 - 4r_{q'}^2} - \hat{q}^2 + 2r_{q'}^2}{2r_{q'}^2}\right) + 2 - \log\left(\frac{m_{q'}^2}{\mu^2}\right) + \frac{1}{\epsilon} + \log(4\pi) - \gamma_E, \quad (\text{B22})$$

$$B_0(m_q^2, m_{q'}^2, m_b^2) = \sqrt{\lambda(x_q^2, x_b^2, x_{q'}^2)} \log\left(\frac{\sqrt{\lambda(x_q^2, x_b^2, x_{q'}^2)} + (r_b^2 + r_{q'}^2 - 1)}{2r_b r_{q'}}\right) + \frac{1}{2} (1 - r_b^2 + r_{q'}^2) \log\left(\frac{r_b^2}{r_{q'}^2}\right) + 2 - \log\left(\frac{m_b^2}{\mu^2}\right) + \frac{1}{\epsilon} + \log(4\pi) - \gamma_E, \quad (\text{B23})$$

where $\lambda(x, y, z) = x^2 + y^2 + z^2 - 2(xy - xz - yz)$. The scale μ and the pole ϵ of dimensional regularization cancel out in our results.

-
- [1] P. Zyla et al. (Particle Data Group), PTEP **2020**, 083C01 (2020).
 - [2] V. Khachatryan et al. (CMS), Phys. Rev. **D93**, 052007 (2016), 1601.01107.
 - [3] A. M. Sirunyan et al. (CMS) (2019), 1903.11144.
 - [4] A. M. Sirunyan et al. (CMS) (2019), 1907.03729.
 - [5] A. M. Sirunyan et al. (CMS), JHEP **06**, 146 (2020), 1912.09540.
 - [6] E. P. Shabalín, Sov. J. Nucl. Phys. **28**, 75 (1978), [Yad. Fiz.28,151(1978)].
 - [7] A. Czarnecki and B. Krause, Phys. Rev. Lett. **78**, 4339 (1997), hep-ph/9704355.
 - [8] I. B. Khriplovich, Phys. Lett. **B173**, 193 (1986), [Yad. Fiz.44,1019(1986)].
 - [9] R. Martinez, M. A. Perez, and N. Poveda, Eur. Phys. J. **C53**, 221 (2008), hep-ph/0701098.
 - [10] I. D. Choudhury and A. Lahiri, Mod. Phys. Lett. **A30**, 1550113 (2015), 1409.0073.
 - [11] J. I. Aranda, D. Espinosa-Gómez, J. Montaña, B. Quezadas-Vivian, F. Ramírez-Zavaleta, and E. S. Tututi, Phys. Rev. **D98**, 116003 (2018), 1809.02817.
 - [12] A. Hernández-Juárez, G. Tavares-Velasco, and A. Moyotl, e-print arxiv: 2009.11955 [hep-ph] (2020), 2009.11955.
 - [13] J. Aranda, T. Cisneros-Pérez, J. Montaña, B. Quezadas-Vivian, F. Ramírez-Zavaleta, and E. Tututi, e-print arxiv: 2009.05195 [hep-ph] (2020), 2009.05195.
 - [14] R. Gaitan, E. A. Garces, J. H. M. de Oca, and R. Martinez, Phys. Rev. **D92**, 094025 (2015), 1505.04168.
 - [15] A. I. Hernández-Juárez, A. Moyotl, and G. Tavares-Velasco, Phys. Rev. **D98**, 035040 (2018), 1805.00615.
 - [16] Q.-H. Cao, C.-R. Chen, F. Larios, and C. P. Yuan, Phys. Rev. **D79**, 015004 (2009), 0801.2998.
 - [17] L. Ding and C.-X. Yue, Commun. Theor. Phys. **50**, 441 (2008), 0801.1880.
 - [18] A. Aboubrahim, T. Ibrahim, P. Nath, and A. Zorik, Phys. Rev. **D92**, 035013 (2015), 1507.02668.
 - [19] R. Martinez, M. A. Perez, and O. A. Sampayo, Int. J. Mod. Phys. **A25**, 1061 (2010), 0805.0371.
 - [20] T. Ibrahim and P. Nath, Phys. Rev. **D84**, 015003 (2011), 1104.3851.
 - [21] J. Ferreira, J.G., P. Pinheiro, C. S. Pires, and P. da Silva, Phys. Rev. D **84**, 095019 (2011), 1109.0031.
 - [22] B. W. Lee and S. Weinberg, Phys. Rev. Lett. **38**, 1237 (1977).
 - [23] F. Pisano and V. Pleitez, Physical Review D **46**, 410 (1992), ISSN 0556-2821, URL <http://dx.doi.org/10.1103/PhysRevD.46.410>.
 - [24] P. H. Frampton, Physical Review Letters **69**, 2889 (1992), ISSN 0031-9007, URL <http://dx.doi.org/10.1103/PhysRevLett.69.2889>.
 - [25] J. Ruiz-Alvarez, C. de S.Pires, F. S. Queiroz, D. Restrepo, and P. Rodrigues da Silva, Phys. Rev. D **86**, 075011 (2012), 1206.5779.
 - [26] C. Kelso, C. A. de S. Pires, S. Profumo, F. S. Queiroz, and P. S. Rodrigues da Silva, Eur. Phys. J. C **74**, 2797 (2014), 1308.6630.
 - [27] E. Ramirez Barreto, Y. Coutinho, and J. Sa Borges, Phys. Rev. D **83**, 075001 (2011), 1103.1267.
 - [28] E. Ramirez Barreto, Y. Coutinho, and J. Sa Borges, Phys. Lett. B **689**, 36 (2010), 1004.3269.
 - [29] E. Ramirez Barreto, Y. Coutinho, and J. Sa Borges, Nucl. Phys. B **810**, 210 (2009), 0811.0846.
 - [30] V. Q. Phong, V. T. Van, and H. N. Long, Phys. Rev. D **88**, 096009 (2013), 1309.0355.
 - [31] D. Cogollo, H. Diniz, C. de S.Pires, and P. Rodrigues da Silva, Eur. Phys. J. C **58**, 455 (2008), 0806.3087.

- [32] F. Queiroz, C. de S.Pires, and P. da Silva, *Phys. Rev. D* **82**, 065018 (2010), 1003.1270.
- [33] W. Caetano, C. A. de S. Pires, P. S. Rodrigues da Silva, D. Cogollo, and F. S. Queiroz, *Eur. Phys. J. C* **73**, 2607 (2013), 1305.7246.
- [34] A. Dias, P. Pinheiro, C. de S.Pires, and P. Rodrigues da Silva, *Annals Phys.* **349**, 232 (2014), 1309.6644.
- [35] J. Ferreira, C. de S.Pires, P. Rodrigues da Silva, and A. Sampieri, *Phys. Rev. D* **88**, 105013 (2013), 1308.0575.
- [36] V. Vien and H. Long, *Int. J. Mod. Phys. A* **28**, 1350159 (2013), 1312.5034.
- [37] V. T. N. Huyen, H. N. Long, T. T. Lam, and V. Q. Phong, *Commun. Phys.* **24**, 97 (2014), 1210.5833.
- [38] D. Cogollo, F. S. Queiroz, and P. Vasconcelos, *Mod. Phys. Lett. A* **29**, 1450173 (2014), 1312.0304.
- [39] C. Kelso, H. Long, R. Martinez, and F. S. Queiroz, *Phys. Rev. D* **90**, 113011 (2014), 1408.6203.
- [40] C. Kelso, P. R. D. Pinheiro, F. S. Queiroz, and W. Shepherd, *The European Physical Journal C* **74** (2014), ISSN 1434-6052, URL <http://dx.doi.org/10.1140/epjc/s10052-014-2808-4>.
- [41] G. De Conto and V. Pleitez, *JHEP* **05**, 104 (2017), 1603.09691.
- [42] M. Tanabashi et al. (Particle Data Group), *Phys. Rev.* **D98**, 030001 (2018).
- [43] A. Machado, J. Montero, and V. Pleitez, *Phys. Rev. D* **88**, 113002 (2013), 1305.1921.
- [44] S. Tatur and J. Bartelski, *Acta Phys. Polon. B* **39**, 2903 (2008), 0801.0095.
- [45] D. Binosi and J. Papavassiliou, *Phys. Rept.* **479**, 1 (2009), 0909.2536.
- [46] A. Denner, G. Weiglein, and S. Dittmaier, *Nucl. Phys. B* **440**, 95 (1995), hep-ph/9410338.
- [47] V. Shtabovenko, R. Mertig, and F. Orellana, *Comput. Phys. Commun.* **207**, 432 (2016), 1601.01167.
- [48] H. H. Patel, *Comput. Phys. Commun.* **197**, 276 (2015), 1503.01469.
- [49] T. Hahn and M. Perez-Victoria, *Comput. Phys. Commun.* **118**, 153 (1999), hep-ph/9807565.
- [50] A. Denner, S. Dittmaier, and L. Hofer, *Comput. Phys. Commun.* **212**, 220 (2017), 1604.06792.